Heliyon 7 (2021) e08248

Contents lists available at ScienceDirect

Heliyon

journal homepage: www.cell.com/heliyon

Research article

Performance enhancement of an FSO link using polarized quasi-diffuse transmitter

Abu Bakarr Sahr Brima [a,*], Edwin Ataro [b], Aladji Kamagate [c]

[a] Department of Electrical Engineering, Pan Africa University Institute for Basic Sciences, Technology, and Innovation (PAUSTI), Juja, Kenya
[b] Department of Electrical & Electronic Engineering, Technical University of Kenya, Nairobi, Kenya
[c] Laboratoire des Sciences et TIC (LASTIC), Ecole Supérieure Africaine des TIC (ESATIC) University, Abidjan, Cote d'Ivoire

ARTICLE INFO

Keywords:
Power divider/holographic beam splitter (hologram)
Quasi-diffused
Polarized
Bit error rate (BER)
Eye height
Maximum quality factor

ABSTRACT

Free space optics (FSO) system has received much interest in recent years as a technology that exhibits cost-effective, better security, license-free, and comprehensive capacity access techniques for transmission of Giga data rate. However, despite all the many advantages demonstrated by its signal, alignment distortion from building sway, atmospheric disturbances from aerosol, scattering, turbulence, and scintillation have shackled the development of the high-speed FSO link and made it less attractive. These atmospheric disturbances have led to the cultivation of spatial diversity techniques for its performance improvement. This work proposes applying a polarized quasi-diffused system with a power divider/holographic beam splitter as a spatial diversity scheme instead of using multiple transmitters. The idea of both analytical and simulation design is considered. The proposed model with power divider/holographic beam splitter has shown a very high maximum quality factor, improved received power, better bit error rate (BER), and eye height depicting the link visibility as compared to the conventional point to point single input single output (SISO) 1TX/RX FSO system for the same transmitted power and link range. The results and data were collected through the help of optisystem software. The obtained results show better performance of an FSO link by using a single transmitter with multi-beam spots from a power divider/hologram instead of using multiple transmitters as a spatial diversity scheme.

1. Introduction

Free space optics (FSO), known as fiber-free or fibreless optics, is an optical communication technique that propagates light in free space, meaning air, outer space, vacuum, or something similar to wireless transmission of data for telecommunication and computer networking [1]. It is a line-of-sight technology that currently enables optical transmission up to 2.5 Gbps of text, video, and voice data through the air at long distances in the order of kilometers, allowing optical connectivity without installing fiber-optic cable or securing spectrum license [2]. FSO can be considered a technology that bridges the existing gap between wireless technology and fiber optics technology with advantages such as high data rate, secure link, cost efficiency, and insusceptibility to electromagnetic interference. The 'last mile' from fiber optic is a challenge in practically laying down the optical fibers and the cost involved. Also, it operates between the 780–1600 nm wavelength bands, which are wavelength/frequency bands of interest in telecommunications. It is a technology that requires low divergence optical signals, which can be produced by using either light-emitting diodes (LEDs) or lasers (light amplification by stimulated emission of radiation) [3]. With all the advantages, it is essential to know that FSO system can encounter significant losses during the transmission process due to in-homogeneities in the atmospheric contents (molecules or particles) and adverse weather conditions. Hence, spatial diversity techniques have been proposed as a breakthrough to facilitate a high data rate with acceptable performance [4].

Salah Mahdi Hamzah and Ibrahim A. Murdas et al. [5] proposed a system that combines dense wavelength division multiplexing (DWDM) and multiple-input multiple-output (MIMO) techniques. The authors used a fork component as a source of multiple transmitters to produce a prototype transmission system to transmit optical signals through the atmosphere with more minor atmospheric disturbances by mitigating the attenuations during the transmission process. The method improved transmission range and signaled quality when using the DWDM-MIMO technique compared to combines dense wavelength division multiplexing single input single output (DWDM-SISO). The

* Corresponding author.
E-mail address: brima.abu@students.jkuat.ac.ke (A.B. Sahr Brima).

https://doi.org/10.1016/j.heliyon.2021.e08248
Received 10 August 2021; Received in revised form 31 August 2021; Accepted 21 October 2021

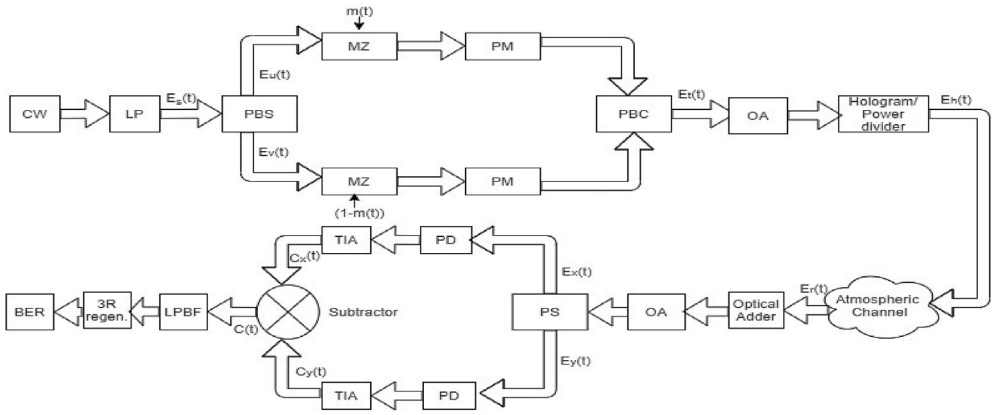

Figure 1. The Block Diagram of the Proposed Polarized Quasi Diffused FSO System Model with Hologram/power divider.

number of transmitters used in the DWDM-MIMO influenced the difference. In [6], the authors investigate the maximum transmission range at a bit rate of 10 Gb/s and quality factor for FSO orthogonal frequency division multiplexing (OFDM) system. The use of DWDM-OFDM as a spatial diversity technique with dual-polarization was analyzed to monitor the performance of the FSO system under the effect of atmospheric attenuation, which serves as a factor limiting the propagation of the optical signal. The investigation shows improved transmission range and quality factor for the FSO-OFDM system, but the implementation is practically shaking. Also, in [7], the authors proposed an FSO optical relaying assisted transmission to increase the link range and optimize the BER. The method proposed processes and a forward optical signal transmitted at intermediate relaying nodes. The simulation and experiment investigating the performance of optical amplify and forward (OAF) relaying shows that differential phase shifting keying (DPSK) with a balanced receiver has a 3dB receiving sensitivity advantage over on-off keying (OOK). However, the OAF relaying node is adopted to extend the FSO transmission distance, but atmospheric attenuations were neglected. [8], the authors analyzed the use of the multiple-input multiple-output (MIMO) technique to mitigate the adverse effect on the FSO system with turbulent atmospheric channels using multiple laser sources and multiple optical detectors. The analysis shows that increasing the number of transmitters increases the system performance, neglecting the undesirable increase in system noise due to the number of transmitters and receivers added. Therefore, the novelty of polarized quasi diffused system technique is to use two or more orthogonal polarizations to carry optical signal in free space through different defined paths simultaneously with the use of power divider/holographic beam splitter, designed to give multi-beam spots from one source instead of using multiple transmitters or receivers, serving as additional sources of system noise. Also, the polarized diffuse system radiates optical power over a wide solid angle to ease the pointing error and shadowing effects of point-to-point FSO links. The transmitter does not need to aim at the receiver since the radiant optical power is assumed to radiate in different directions towards the receiver. Hence, the diffuse channel does not exhibit fading because the receiver photodiode detectors integrate the optical intensity field over an area of million square wavelengths. This leads to no change in the channel response even if the photodiode is moved a distance in the order of the wavelength.

2. Methodology analysis

2.1. Proposed polarized quasi-diffused system model

The block diagram of the proposed model, whose theoretical analysis is discussed below, is represented in Figure 1. The analysis followed step-by-step modeling of the system.

Where; LP stands for a linear polarizer, CW is a continuous-wave laser, PBS is a polarization beam splitter, MZ is Mach-Zehnder modulator, PM is phase modulator, PBC represent polarization beam combiner, PD is photodiode detector, BER is bit error rate analyzer, LPBF is low pass Bessel filter, OA stands for optical amplifier and TIA represent transimpedance amplifier. In the software, the power divider represents the holographic beam splitter, shown in Figure 1. In practical cases, a hologram is a unique computer-generated holographic device (CGH) that represents a sort of diffraction grating with a fringe bifurcation forming the "fork" structure [9].

2.2. Transmitting units

The proposed polarized quasi diffused transmitter comprises the following components:

i. Pseudorandom bit sequence generator gives the data information to be transmitted.
ii. Beam splitter.
iii. The non-Return to Zero (NRZ) component generates the non-return to zero code signals.
iv. Mach Zehnder (MZ) optical modulator modifies the intensity of the output light signal from the PBS.
v. Power divider/holographic beam splitter divides the input signal into several output signals.
vi. CW Laser generates the power to transmit the light signal
vii. Linear Polarizer polarizes the light from the laser into two orthogonal components.

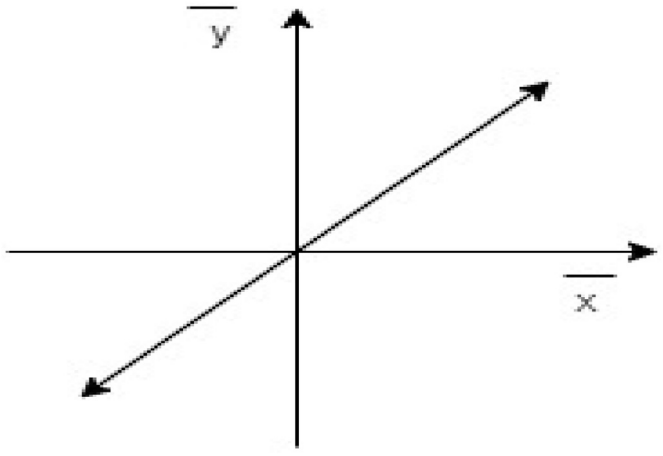

Figure 2. Field configuration of a linearly polarized wave.

viii. Phase modulator (PM), used to modulate the optical light signal.

For a laser beam propagating over an atmospheric channel, the polarization is considered the most stable characteristic of all parameters [10]. The field amplitude is projected along the horizontal $\bar{x}$ and vertical $\bar{y}$ axes as shown in Figure 2 and can be described by the parametric equations as:

$$\overline{E}_x = A_x exp^{j(w(t)-k_z)}\overline{x} \tag{1}$$

$$\overline{E}_y = A_y exp^{j(w(t)-k_{z+\varphi})}\overline{y} \tag{2}$$

where: A_x and A_y correspond to the amplitude of the electric field projected on the $\bar{x}$ and $\bar{y}$-axis, respectively. φ stands for the phase difference between $\overline{E}_x$ and $\overline{E}_y$, which yields the shape of the electric field. The light is linearly polarized along the $\bar{x}$ or $\bar{y}$-axis if the A_x or A_y component is zero and the phase difference is 0 or π. In this work, we assumed that the light is linearly polarized along the $\bar{x}$-axis given a phase difference of zero, and it gave the transmitted signal by:

$$\overline{E}_s(t) = \sqrt{\frac{P_T}{2}} exp^{j[w(t)+\varphi_s(t)]} \tag{3}$$

Considering the effect of a balanced 50/50, two beams splitter [11], as shown in Figure 3.Where; 'u' and 'v' are transmitted optical components of the splitter signals in 'u' and 'v' directions, respectively.

$$\overline{E}_z(t) = |u||v| exp^{j(\varphi_v-\varphi_u)} + |u||v| exp^{-j(\varphi_v-\varphi_u)} \tag{4}$$

$$= 2cos(\varphi_v - \varphi_u) = 0$$

$$\varphi_v - \varphi_u = \frac{\pi}{2}$$

In this paper, we assumed $\varphi_u = 0$, which implies. $\varphi_v = \frac{\pi}{2}$

Invoking the analysis to the block diagram, the applied signal from the linear polarizer is decomposed into two orthogonal components with equal amplitude by the polarization beam splitter. The decomposed optical signals along the U and V axes of the PBS is given as [10]:

$$\overline{E}_s(t) = \overline{E}_u(t) + \overline{E}_v(t) \tag{5}$$

where;

$$\overline{E}_u(t) = \sqrt{\frac{P_T}{2}} exp^{j[w(t)+\varphi_s(t)]}\widehat{u} \tag{6}$$

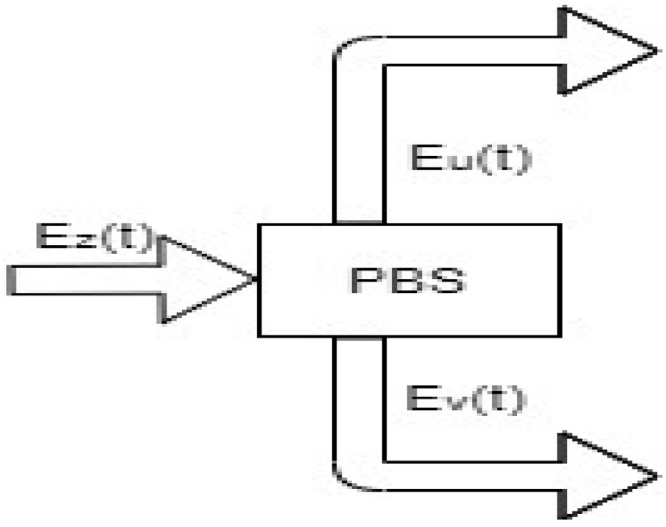

Figure 3. Configuration of a balanced 50/50 beam splitter.

$$\overline{E}_v(t) = \sqrt{\frac{P_T}{2}} exp^{j[w(t)+\varphi_s(t)]}\widehat{v} \tag{7}$$

The emitted electrical field of the optical carrier $\overline{E}_s(t)$ linearly polarized is split equally by the PBS and fed into two identical Mach Zehnder (MZ) modulators that hold the information bits. At the output of each MZ, the optical signals will experience both constructive and destructive patterns depending on the phase difference of 0 and $\frac{\pi}{2}$, respectively.

Hence the transmitted optical field at the output of the polarization beam combiner is expressed by [12];

$$\overline{E}_t(t) = \sqrt{\frac{P_T}{2}} exp^{(w(t)+\varphi_t(t)+\gamma)}\{m(t)\widehat{u} + (1-m(t)\widehat{v}\} \tag{8}$$

where; γ is the modulation function, $\gamma \in (0, \pi)$ for $b_k \in (1, 0)$ The vector $m(t)$ is expressed as;

$$m(t) = \sum_{k=-\infty}^{\infty} b_k rect_T(t - kT) \tag{9}$$

where: $b_k = (0, 1) =$ transmitted bit, T represents symbol period, and rectangular pulse shaping function and $rect_T(t)$ denotes the rectangular pulse shaping function and is equal to one (1) for $t \in (0, \pi)$ and zero elsewhere. The hologram/power divider then splits the beam into several beams $(N_t = 1, 2, \ldots\ldots N)$ each with a characteristic of the original beam except for its power and angle of propagation. In this work, we used two plane-polarized spatially coherent waves at the input of the power divider/holographic beam splitter to create sinusoidal interference, giving the transmittance of the hologram towards the optical adder as;

$$\overline{E}_h(t) = \frac{1}{N_t}\sum_{i=1}^{N_t=4} S_{Zi} \tag{10}$$

where S_Z represents the spot size and is given by [13]:

$$S_Z = \frac{4D\lambda}{\pi x}\,\overline{E}_t(t) \tag{11}$$

giving the transmittance of the hologram as:

$$\overline{E}_h(t) = \frac{1}{N_t}\sum_{i=1}^{N_t=4}\frac{4D\lambda}{\pi x}\left(\sqrt{\frac{P_{Ti}}{2}} exp^{(w(t)+\varphi_t(t)+\gamma)}\{m(t)\widehat{u} + (1-m(t)\widehat{v}\}\right) \tag{12}$$

where:

S_z = spot size
x = input beam size
λ = wavelength
D = working distance and is related to the inter-spot distance by
d = $Dtan\theta_s$
d = distance between diffracted spots (inter-spot distance) and the optical axis
θ_s = angle between diffracted spots and the optical axis.

Note, the input beam size is determined by various design parameters specific to the application at hand and is usually at least three times the size of the period in the diffractive optical element (DOE). The period in the DOE is given by [13]:

$$\Lambda = \frac{m\lambda}{\sin\alpha} \tag{13}$$

where;

Λ = period of DOE
m = diffractive order
λ = wavelength
α = separation angle between beams

2.3. Channel model

The primary impairment in FSO system communication considering the propagation channel is the turbulence-induced fading. Experimental studies have shown that the lognormal distribution can be used to statistically characterize the fading in the FSO system in weak atmospheric turbulence conditions. In other words, the lognormal model is a statistical model proposed to describe irradiance fluctuation in FSO system under weak turbulence conditions. Hence in this work, we configured the FSO channel in the optisystem software to obey the lognormal channel model for the laser wave propagating through the channel.

Therefore, invoking the variable transformation, the lognormal Probability density function (PDF) can be given by [14]:

$$P(I)=\frac{1}{\sqrt{2\pi\sigma_l I}}exp\left(-\frac{\left(\ln I+\sigma_l{}^2/2\right)^2}{2\sigma_l{}^2}\right),\ I>0 \tag{14}$$

where $I=exp(X)$ is the channel gain, X is the Gaussian Rytov variance (RV) having mean μ and variance $\sigma_l{}^2$, respectively. Also, σ_l is the scintillation level whose typical value is less than 0.5 for FSO system [15].

2.4. Receiving units

The receiving end of the proposed FSO link comprises a polarization splitter, photodiode (PIN), a low-pass filter (Bessel filter), transimpedance amplifier, electrical subtractors, 3R regenerator, and a visualizer (BER analyzer). The photodetectors have a gain of 3dB, each with a responsivity of 0.85A/W and a dark current of around 10nA. An avalanche photodiode (APD) can also be used for long-distance free-space optical data transmission because of its merits of producing high amplification for low or weak light signals. The received signal undergoes further processing steps by passing it through a low pass Bessel filter of the cutoff frequency of 75% of the bit rate to limit its bandwidth. 3R regenerator regenerates the electrical signal of the same original bit sequence. Then, the modulated electrical signal from the 3R generator is expected to be similar to that produced by the transmitter to achieve the optimum BER evaluation. The output of the 3R regenerator is then connected to the BER analyzer, which gives the maximum Q-factor, minimum BER, eye height, and threshold.

Following the process from Eq. (12) of the hologram/power divider, the received optical beams at the optical adder is given by;

$$\overline{E}_r(t)=\frac{1}{N_t}\sum_{i=1}^{N_t=4}\frac{4D\lambda}{\pi x}\left(\sqrt{\frac{P_{Ri}}{2}}exp^{(w(t)+\varphi_r(t)+\gamma)}\{m(t)\widehat{u}+(1-m(t)\widehat{v}\}\right) \tag{15}$$

where;

$$P_R=\frac{d_r{}^2}{[\,d_t+(L\theta)]^2}P_T\ e^{-\alpha L}$$

[16] d_r is the diameter of the receiver aperture (m), d_t is the diameter of transmitter aperture (m), θ is the beam divergence (mrad), P_R = received power, P_T = transmitted power, L = link range, α = coefficient of attenuation and φ_r= phase noise of receiver.

The term $\frac{1}{N_t}$ is added to ensure that the overall power conforms to conventional single input single output (SISO) TX/RX FSO system [17]. The received signal is superimposed onto the polarization splitter (PS) and passes through to the optical adder receiver. Then the optical orthogonal signals are decomposed into two received signals $\overline{E}_x(t)$ and $\overline{E}_y(t)$ given by [10]:

$$\overline{E}_x(t)=\frac{1}{N_t}\sum_{i=1}^{N_t=4}\frac{4D\lambda}{\pi x}\left(\sqrt{\frac{P_{Ti}}{2}}exp^{(w(t)+\varphi_r(t)+\gamma)}\{m(t)\widehat{u}\}\right) \tag{16}$$

$$\overline{E}_y(t)=\frac{1}{N_t}\sum_{i=1}^{N_t=4}\frac{4D\lambda}{\pi x}\left(\sqrt{\frac{P_{Ti}}{2}}exp^{(w(t)+\varphi_r(t)+\gamma)}\{(1-m(t)\widehat{v}\}\right) \tag{17}$$

Hence, the photodetectors detect the output sum from the polarization beam splitter optical fields of the two orthogonal signals and provide an electrical current proportional to the received optical power. The output of the two photodetectors followed by TIA each is connected to a single input low pass Bessel filter. Following the optical to electrical signal conversion, the signals $c_x(t)$ and $c_y(t)$ at the output of the two identical PIN photodiode (PD) detectors are expressed by [12]:

$$C_x(t)=\left\{\frac{1}{N_t}\sum_{i=1}^{N_t=4}R\frac{4D\lambda}{\pi x}\eta\left|\sqrt{\frac{P_{Ri}}{2}}\right|^2 m(t)\right\}+n_x(t) \tag{18}$$

$$C_y(t)=\left\{\frac{1}{N_t}\sum_{i=1}^{N_t=4}R\frac{4D\lambda}{\pi x}\eta\left|\sqrt{\frac{P_{Ri}}{2}}\right|^2 (1-m(t))\right\}+n_y(t) \tag{19}$$

where: R stands for the responsivity of the photodiode, $n_x(t)$ and $n_y(t)$ represents the background radiation and thermal noise, also known as system noise terms which are assumed to be statistically independent and are modeled as AWGN with zero means and variance $\sigma_n{}^2=\frac{1}{2}N_o$, with N_o standing for double-sided noise power spectral density representing the background noise and thermal noise. η denotes the optical efficiency for the two-beam splitter given by [13]:

$$\eta=\frac{8}{\pi^2} \tag{20}$$

We assumed an undistorted signal, giving the detector output to be:

$$C_x(t)=\left(R\frac{4D\lambda P_R}{2\pi x}\eta\right)m(t)+n_x(t) \tag{21}$$

$$C_y(t)=\left(R\frac{4D\lambda P_R}{2\pi x}\eta\right)(1-m(t))+n_y(t) \tag{22}$$

Hence the instantaneous electrical signal of the subtractor is given by [10]:

$$C(t)=C_x(t)-C_y(t) \tag{23}$$

$$C(t)=\frac{2\lambda RD\eta P_R}{\pi x}(2m(t)-1)+n(t) \tag{24}$$

where $n(t)$ is the zero Gaussian with variance $\frac{\sigma_n{}^2}{2}$. The output signal is then transferred to a low-pass Bessel filter with a bandwidth equal to the bit rate. The Bessel filter has a transfer function given by [18]:

$$H(s)=\frac{\alpha d_0}{B_N(s)} \tag{25}$$

where: α is the parameter insertion loss, N is the parameter order.

$d_0=\frac{2N}{2^N N!}$ being the normalizing constant and.

$B_N(s)$ is the nth order Bessel polynomial of the form given by:

$B_N(s)=\sum_{k=0}^{N}d_k S^k d_k=\frac{(2N-k)!}{2^{N-k}k!(N-k)!}$, $S=j\left(\frac{f^* w_b}{f_c}\right)$ for f_c being the filter cutoff frequency defined by the parameter frequency and w_b denotes the normalized 3dB, which can be approximated as:

$$w_b\approx\sqrt{(2N-1)\ln 2}$$

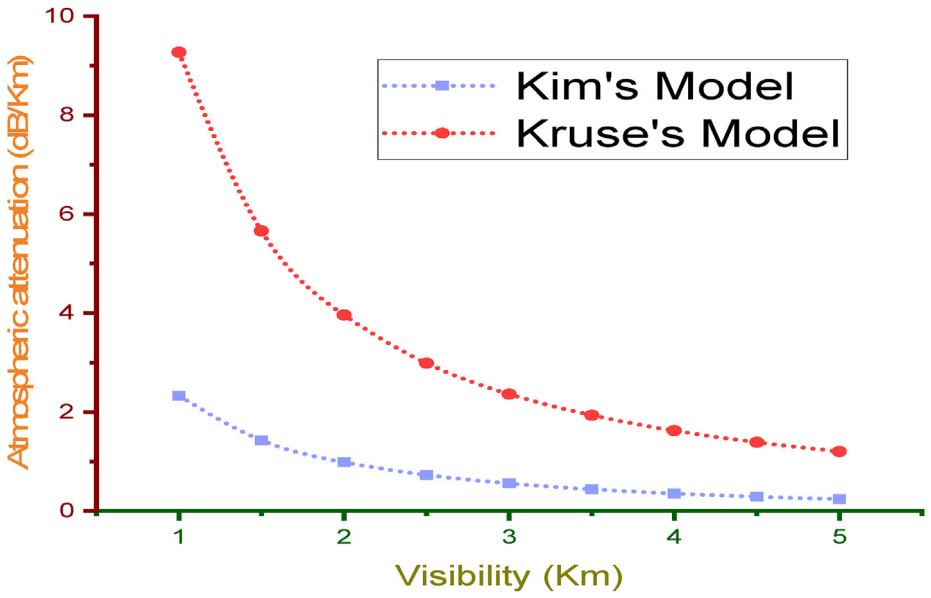

Figure 4. Atmospheric Attenuation (dB/km) versus visibility (km).

Therefore, the output from the low pass Bessel filter is defined by [10]:

$$v_i = \frac{1}{T}\int_0^T c(t)^* h_{LBF}(t) = \begin{cases} -\frac{2R\lambda D\eta P_R}{\pi x} + n_{LBF}\ for\ m(t) = 0 \\ \frac{2R\lambda D\eta P_R}{\pi x} + n_{LBF}\ for\ m(t) = 1 \end{cases} \quad (26)$$

where: T is the symbol period, $c(t)$ is the output signal of the subtractor, $h_{LBF}(t)$ is the impulse response of the low pass Bessel filter, and $n_{LBF} \sim \left[0, \frac{\sigma_n^2}{2}\right]$ is the white Gaussian noise.

A decision is made in favor of the amplitude level close to v_i, which is monitored within the range of $b_{on} = \frac{2R\lambda D\eta P_R}{\pi x}$ and $b_{off} = -\frac{2R\lambda D\eta P_R}{\pi x}$ for the transmission of '1' and '0' respectively.

Assuming independent and identical distributed transmission, meaning the signal level is balanced on the time axis, and the spectrum is transformed by filtering to a white noise signal or a signal where all frequencies are equally present, the probability density function of the instantaneous SNR (error probability) is given by [8].

$$F(v) = \frac{1}{\sqrt{2\pi{\sigma_n}^2}}\int_0^\infty exp\left(-\frac{(v-m)^2}{2{\sigma_n}^2}\right)dv \quad (27)$$

where F(v) is the probability density function, ${\sigma_n}^2$ and σ_n are the noise variance and standard deviation, respectively.

Hence the probability density function which is used to determine the error probability in an FSO system in which the logic 1 pulses all of amplitude v for a Gaussian output with mean and variance of b_{on} and ${\sigma_{on}}^2$ respectively, is given by [8]:

$$P_1(v_{th}) = \frac{1}{\sqrt{2\pi{\sigma_{on}}^2}}\int_{-\infty}^{v_{th}} exp\left(-\frac{(b_{on}-v)^2}{2{\sigma_n}^2}\right)dv \quad (28)$$

Similarly, for logic 0 pulses, all amplitude v (no pulse register at the decoding time) has a mean and variance of b_{off} and ${\sigma_{off}}^2$, respectively. The probability of error is equal to the probability that the noise will exceed the threshold voltage, which is mistaken for a 1 pulse is given by:

$$P_o(v_{th}) = \frac{1}{\sqrt{2\pi{\sigma_{off}}^2}}\int_{v_{th}}^\infty exp\left(-\frac{(v-b_{off})^2}{2{\sigma_n}^2}\right)dv \quad (29)$$

where $P_1(v_{th})$ and $P_o(v_{th})$ denote the probability of error in the presence of 1 bit and 0 bit, respectively.

The total error probability is given by:

$$F(V) = \frac{1}{2}P_1(v_{th}) + \frac{1}{2}P_0(v_{th}) \quad (30)$$

If assumed that the probability of 0 and 1 pulse are equally likely, then the BER becomes [8]:

$$BER = \frac{1}{\sqrt{2\pi}}\left(\frac{\exp\left(Q^2/2\right)}{Q}\right) \quad (31)$$

where $Q = \frac{v_{th}-b_{off}}{\sigma_{off}} = \frac{b_{on}-v_{th}}{\sigma_{on}} = \frac{b_{on}-b_{off}}{\sigma_{on}+\sigma_{off}}$

The average BER condition on the received irradiance for FSO signal propagating through the turbulence lognormal channel can be obtained as [17]:

$$BER = \frac{1}{\sqrt{2\pi{\sigma_n}^2}}\int_0^{v_{th}}\int_0^\infty exp\left(-\frac{\left(v-\frac{2R\lambda D\eta P_R}{\pi x}\right)^2}{{\sigma_n}^2}\right)P(I)dvdI \quad (32)$$

Performing some mathematical expression transformation, the BER can be further expressed as:

$$BER = \frac{1}{2}\left(erfc\left(\frac{\left|b_{on}-v_{th}\right|}{\sigma_{on}}\right) + erfc\left(\frac{\left|v_{th}-b_{off}\right|}{\sigma_{off}}\right)\right) \quad (33)$$

$$BER = \frac{1}{2}erfc\left(\frac{2R\lambda D\eta P_R}{\pi x\sigma_n}\right) \quad (34)$$

The closed-form approximation is given by:

$$BER = \frac{1}{2}erfc\left(\frac{Q}{\sqrt{2}}\right) \quad (35)$$

where $Q = \frac{2\sqrt{2}R\lambda D\eta P_R}{\pi x\sigma_n}$ represent the average optical signal-to-noise ratio.

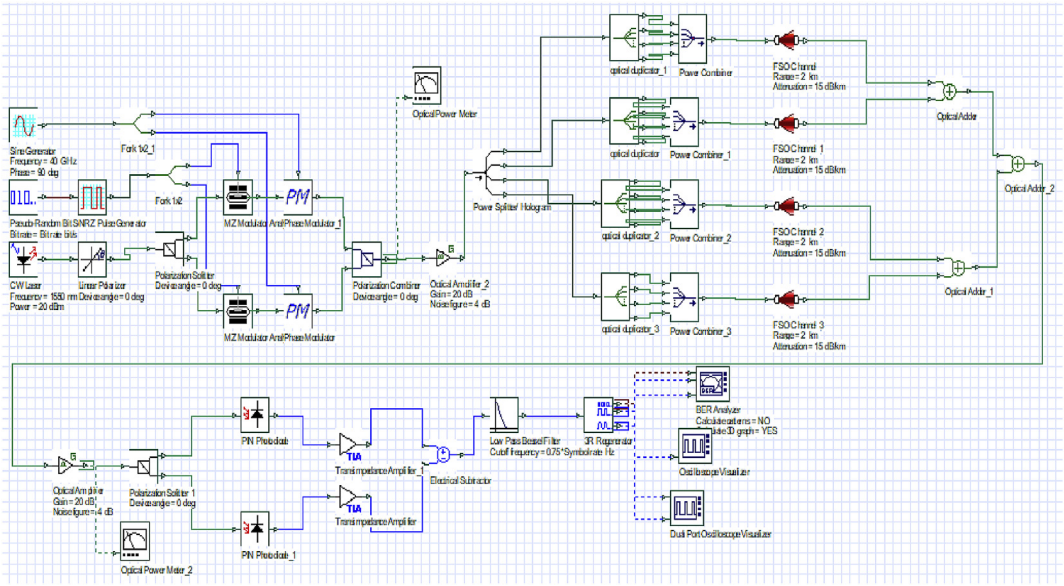

Figure 5. Simulation schematic layout of the proposed polarized quasi-diffused FSO system with hologram/power divider.

2.5. FSO link challenges

One of the major impairments of the FSO link, which may lead to signal degradation and system failure, is atmospheric attenuation which usually occurs due to aerosol/absorption and scattering. The major causes of these attenuations are snow, fog, rain, and dust. The most common is fog attenuation, formed because of the condensation of water vapors present in the atmosphere. Hence fog attenuation can be predicted depending on the size of the atmospheric particles, visibility of the link, and the type of scattering. Visibility can be considered as the degree to which things may be seen. Therefore, according to Kim's model [19], atmospheric attenuation can be given by;

$$\text{Coefficient of atmospheric attenuation}(\alpha) = \frac{3.9120}{V} \cdot \left(\frac{\lambda}{550}\right)^{-q} \tag{36}$$

where: V is visibility (km), q is the size of scattering particles, and λ is the wavelength (*nm*). Kim's model allows the parameter q to take different values which varied according to various weather conditions.

$$q = \begin{cases} 1.6 & \textit{for high visibility } (v > 50km) \\ 1.3 & \textit{for average visibility } (6km < v < 50km) \\ 0.16v + 0.34 & \textit{for haze visibility } (1km < v < 6km) \\ v - 0.15 & \textit{for mist visibility } (0.5km < v < 1km) \\ 0 & \textit{for fog visibility } (v < 0.5km) \end{cases} \tag{37}$$

For Kruse model,

$$\alpha_e\left(dB/km\right) = \frac{17}{V(km)} \left(\frac{0.55}{\lambda(\mu m)}\right)^{q} \geq 0 \tag{38}$$

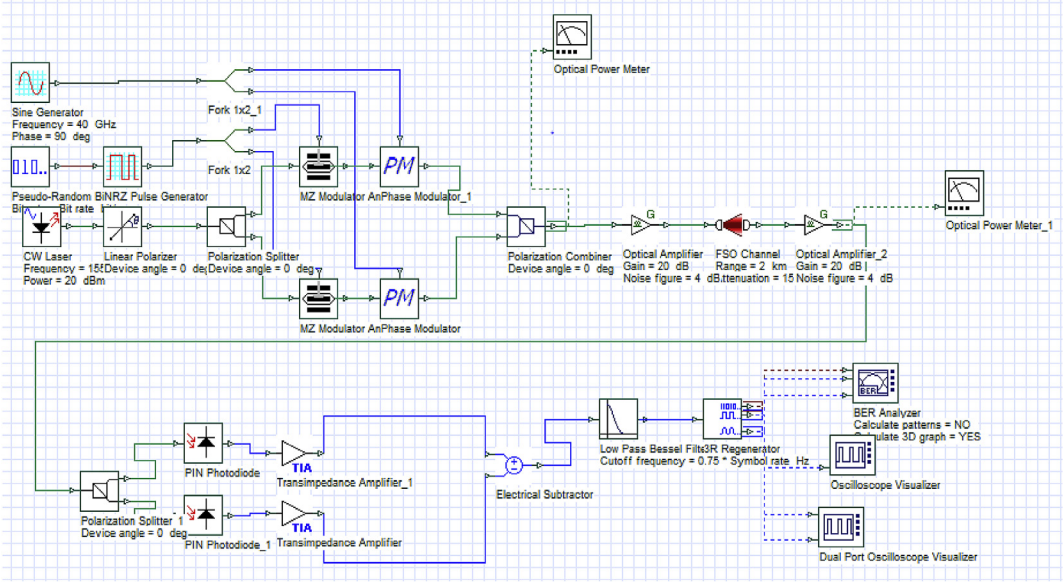

Figure 6. Simulation schematic layout of the polarized system without hologram/power divider.

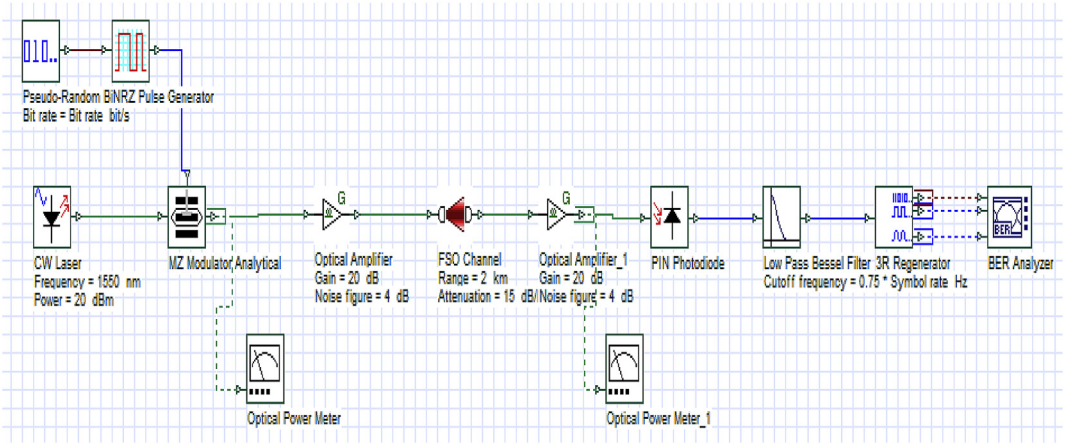

Figure 7. Simulation schematic layout of the conventional single input single output (SISO) TX/RX FSO system model.

$$q = \begin{cases} 1.6 & v > 50km \\ 1.3 & 6km < v < 50km \\ 0.585V^{\frac{1}{3}} & v < 6km \end{cases} \quad (39)$$

Therefore, for different weather conditions, this research work calculates the attenuation value using a transmitting signal of 1550nm (wavelength of atmospheric transmission window) at a distance L (km). Moreover, in this research, Kruse's model is considered for the various attenuation calculations because of its clear advantage of giving better atmospheric attenuation approximation over Kim's model, as shown in Figure 4.

3. Proposed system simulation design

FSO system comprises the FSO transmitter, FSO channel, and the FSO receiver. In practice, the FSO system experiences different attenuations in different weather. In this work, we consider three atmospheric attenuation conditions. That is, clear, haze, and fog with attenuations values of 0.43 dB/km (i.e. 6Km < visibility(v) < 10km according to Kruse's model), 4.3 dB/km (1Km < V < 6Km) and 7.84 dB/km (0Km < V < 0.5km) respectively with special attention to light fog, because attenuation at this weather condition highly degrades the FSO system performance. The simulation setup for analyzing and characterizing the performance of the proposed polarized quasi diffuse model with hologram/power divider and polarized system without hologram/power divider is shown in Figure 5 and Figure 6, respectively. This simulation considers different visualizers like the power meter with the unit in dBm, BER analyzer, which shows the maximum Q-Factor and minimum bit error rate (Min BER). The proposed system is evaluated by comparing it with the conventional single input single output (SISO) 1TX/RX FSO system, as shown in Figure 7.

Table 1. Simulation parameters of the proposed polarized quasi diffuse FSO transmitter model.

Parameters	Values
Optical frequency	1550nm
CW laser power	20 dBm
Beam divergence	2mrad
FSO channel	Lognormal
Modulator	Mach Zehnder, Phase Modulator
Link range	1–5km
Optical detector Responsivity	PIN 0.85
Filter Type Filter order	Low pass Bessel Filter 4
Polarizer	Linear Polarizer
Hologram/Power splitter	Four spots
Polarization Beam splitter (PBS)	
Polarization Beam combiner (PBC)	
Optical Adder	
3R regenerator BER analyzer	
Data rate	10Gbps
Pseudorandom bit sequence (PBRS)	
Non-return to zero (NRZ)	
trans-impedance amplifier bandwidth	$1GH_z$
Optical amplifier gain	20dB
Transmitter aperture diameter	5cm
Receiver aperture diameter	20cm

3.1. Simulation parameters

.Please refer Table 1.

4. Results and discussion

The work analyzed the performance of the proposed quasi-diffused FSO systems model with hologram/power divider and polarized system without power divider/hologram. Simulation results values for

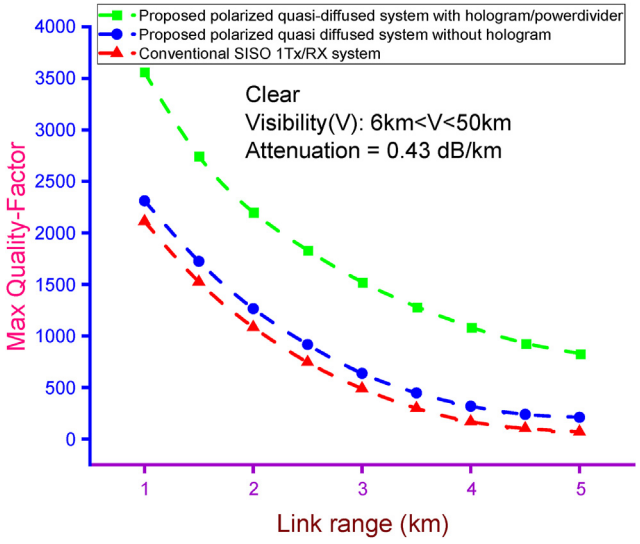

Figure 8. Maximum quality factor versus link Range (km).

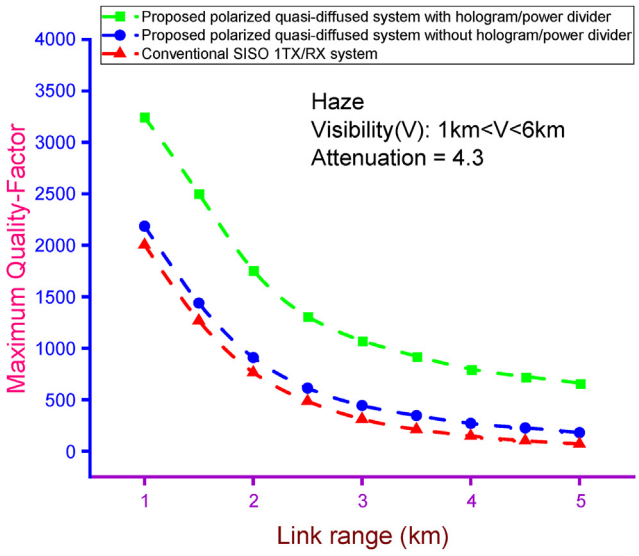

Figure 9. Maximum quality factor versus link range (km).

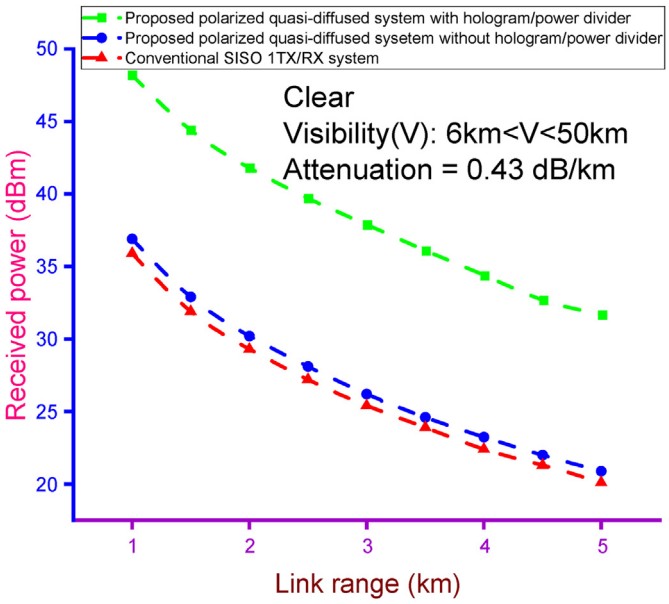

Figure 11. Received Power (dBm) versus link range (km).

maximum Q-factor versus link range is illustrated in Figures 8, 9, and 10. Also received power versus link range, and eye height versus link range for the proposed polarized quasi-diffused FSO system with hologram/power divider and polarized FSO system without power divider/hologram together with the conventional SISO 1TX/RX FSO system are shown in Figures 11, 12 and 13, and Figures 14, 15 and 16, respectively. In order to verify simulations results and system performance, a comparison of the performance of the proposed polarized quasi-diffused FSO system model with power divider/hologram and polarized FSO system without power divider/hologram is made with that of the conventional single input single output (SISO) 1TX/RX FSO system using the same simulation parameters shown in Table 1. Hence the simulation plot for the polarized quasi-diffused FSO system model with hologram/power divider and polarized FSO system without hologram/power divider shows substantial agreement with the conventional SISO 1TX/RX model with the same system parameters. However, under the same atmospheric conditions and system parameters, the performance of the proposed polarized quasi diffused model with power divider/hologram shows a much better performance metric than the conventional SISO 1TX/RX FSO system together with the proposed polarized system without hologram/power divider. In addition, the proposed polarized system's performance without hologram exhibits a slight improvement over the conventional SISO 1TX/RX FSO system.

Table 2 shows min BER versus link range under light fog conditions. Bit error rate (error rate) represents the number of error bits present in the number of received bits of data in a telecommunication system due to distortion, noise, or interference. The bit error rate (BER) depicts the percentage of bits with errors relative to the total received bit in a transmission in communication engineering. Hence as shown in Table 2, min BER for light fog atmospheric conditions with an increase in link range is much appreciable with the proposed polarized quasi-diffuse model with power divider/hologram. And slightly better with the polarized system without power divider/hologram than the conventional SISO 1TX/RX FSO system.

The quality factor (Q-factor) can be considered as a measure of how noisy a pulse is. It provides a quantitative description of receiver

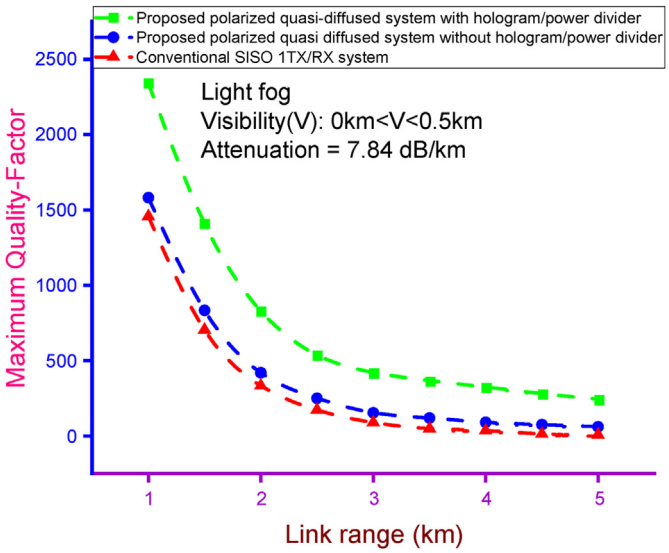

Figure 10. Maximum quality factor versus link range (km).

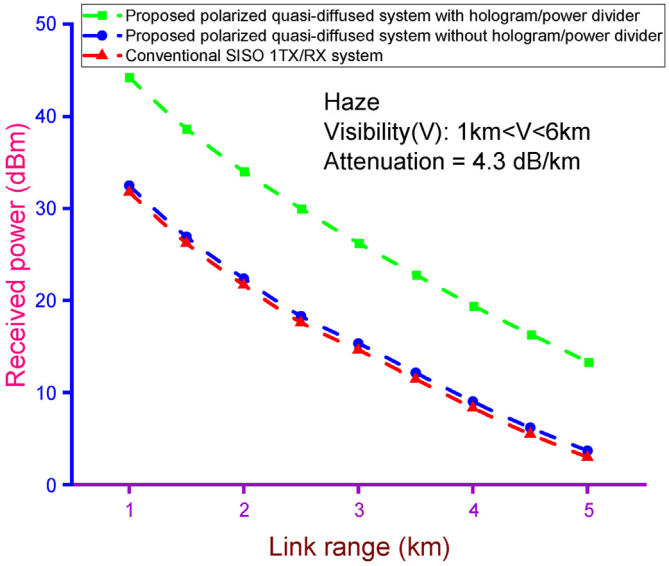

Figure 12. Received power (dBm) versus link range (km).

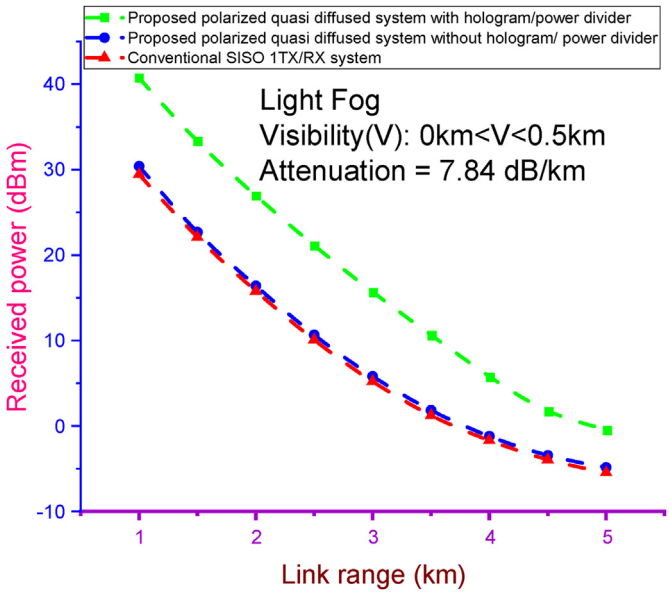

Figure 13. Received power (dBm) versus link range (km).

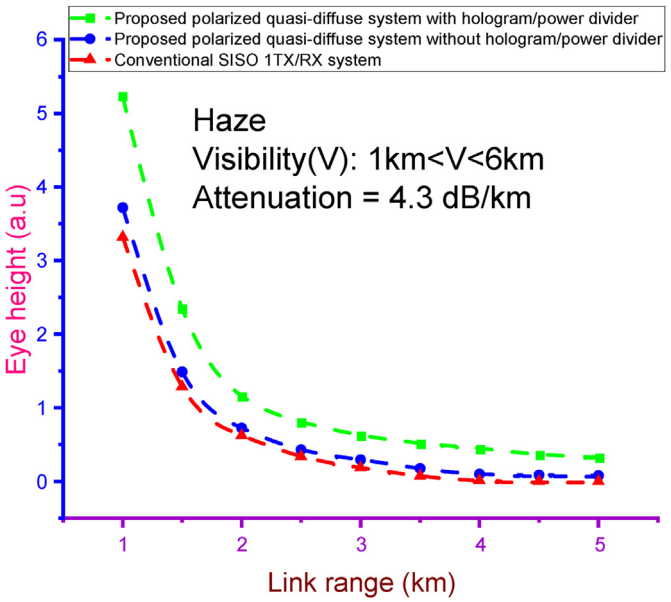

Figure 15. Eye height versus link range (km).

performance. In other words, it takes into consideration the impairment of the transmission signal. Polarization, noise or nonlinear effects, etc., can lead to undesirable signal degradation and ultimately cause high transmission bit error. The quality factor must be high for better system performance, which gives a lower bit error rate (BER). Hence quality factor versus link range (km) for the different attenuations is shown in Figures 8, 9, and 10. From these figures, we can see that the Q-factor plots versus link range for the polarized quasi diffused system with power divider/hologram show a better performance metric than the polarized system without hologram/power divider and that of the conventional SISO 1TX/RX FSO system. Therefore, the proposed polarized quasi diffused system is promising for achieving better Q-factor under the various atmospheric attenuations compared to the polarized system without hologram/power divider and that of the conventional SISO 1TX/RX FSO system.

Figures 11, 12, and 13 show plots of received power (dBm) versus link range (km). The power at the receiver of an FSO system depends on several conditions like the link distance (range), bit rate, wavelength, and atmospheric attenuation. In this research, the results of the received power were calculated at different link ranges and attenuations using the optical transmission window of 1550nm with the help of the power meter, a component in the optisystem software. The received powers versus link range results under three different atmospheric attenuation values for the three systems is shown in Figures 11, 12, and 13. From these figures, it can be seen that the increase in link range for the three systems under the different atmospheric attenuations results in lesser receiver power, which shows degradation in the performance of the system. However, the effect of atmospheric attenuation on the received power for the polarized quasi diffuse model with power divider/hologram is much less severe and slightly less severe with the polarized system without hologram compared to the conventional SISO 1TX/RX FSO model.

The eye height refers to the opening in the eye pattern, which shows the quality of the signal. The more eye-opening, the lesser the error, and therefore better system performance can be achieved. Figures 14, 15, and 16 show the eye height (a.u) versus the link range (km) under clear, haze,

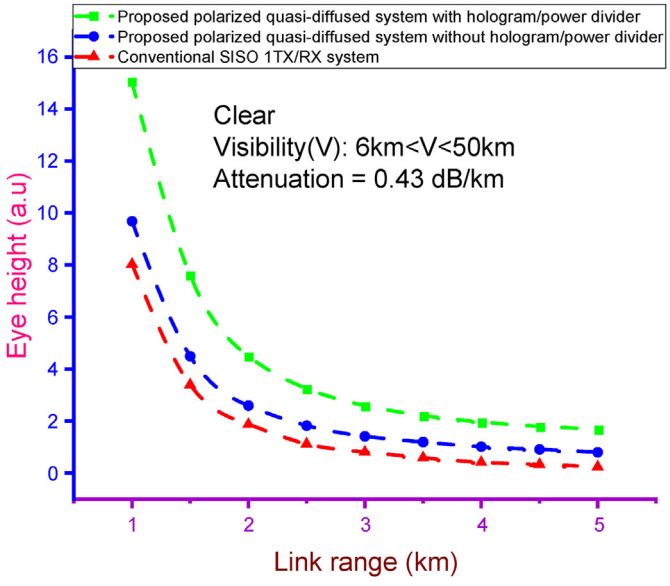

Figure 14. Eye height versus link range (km).

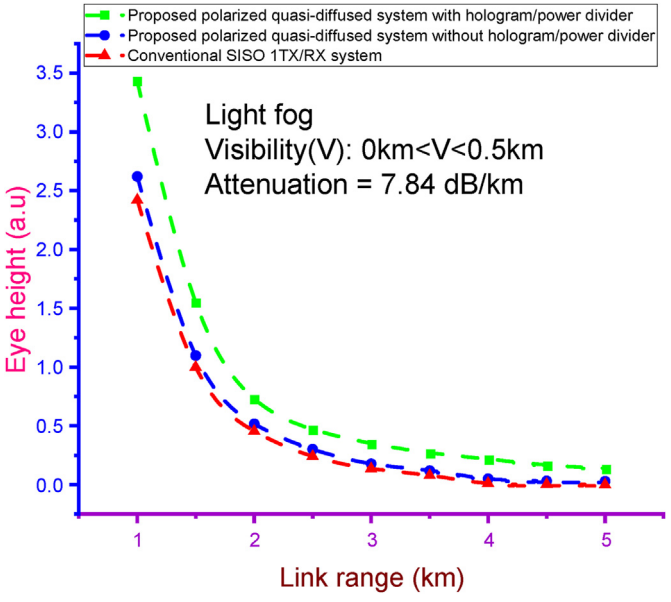

Figure 16. Eye height versus link range (km).

Table 2. Min BER versus link range (km) under light fog condition.

Light Fog condition (Attenuation = 7.84 dB/km)			
Link Range (km)	Proposed Polarized quasi-diffused system with hologram/power divider Min BER	Proposed polarized quasi-diffused system without hologram/power divider Min BER	Conventional SISO 1TX/RX system Min BER
1	0	0	0
1.5	0	0	0
2	0	0	0
2.5	0	0	0
3	0	0	0
3.5	0	0	0
4	0	1.4E-160	2.83E-146
4.5	0	2.6E-60	1.15E-40
5	1.24E-237	4.0E-20	5.87E-12

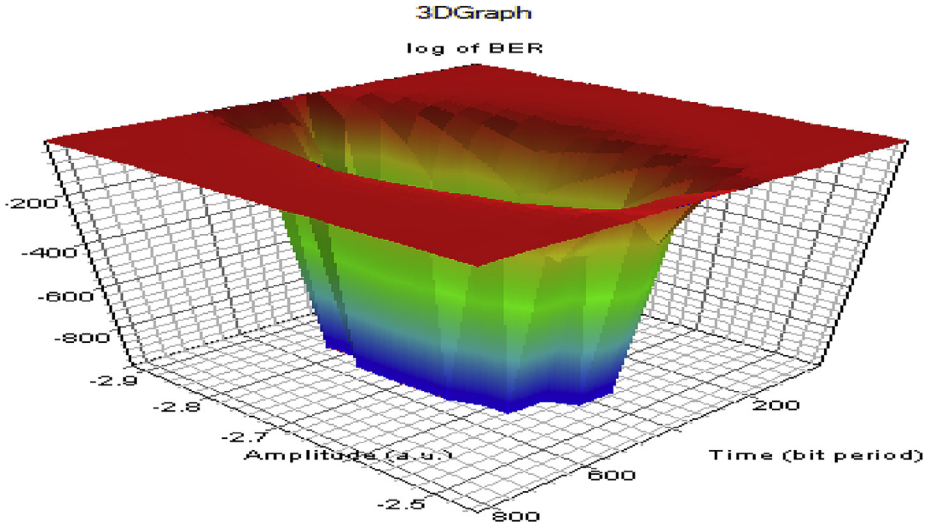

Figure 17. 3D graph of Time (bit period) versus Amplitude (a.u) versus BER of the proposed polarized quasi diffused FSO system with hologram/power divider under light fog condition.

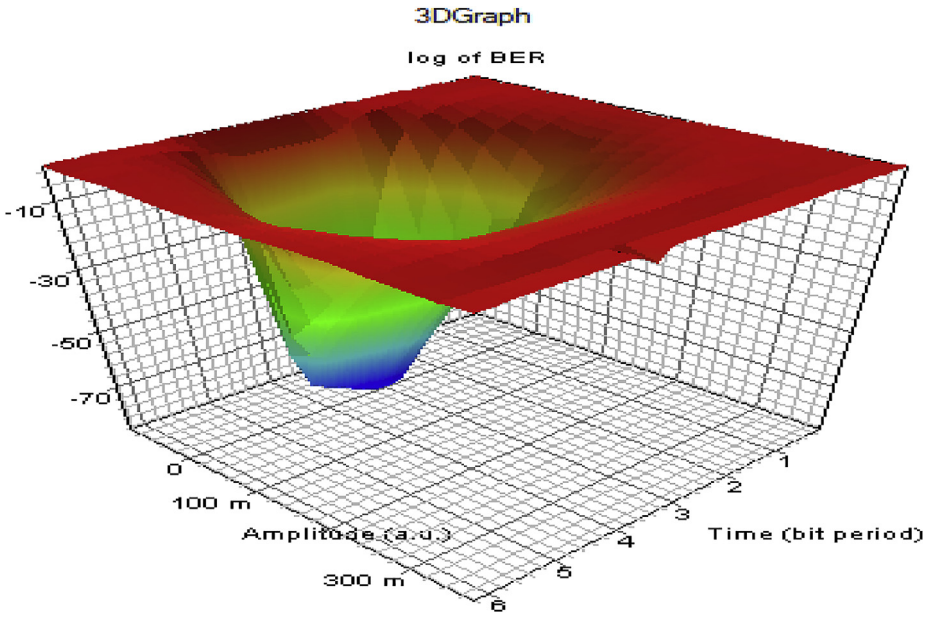

Figure 18. 3D graph of Time (bit period) versus Amplitude (a.u) versus BER of the proposed polarized FSO system without hologram/power divider under light fog condition.

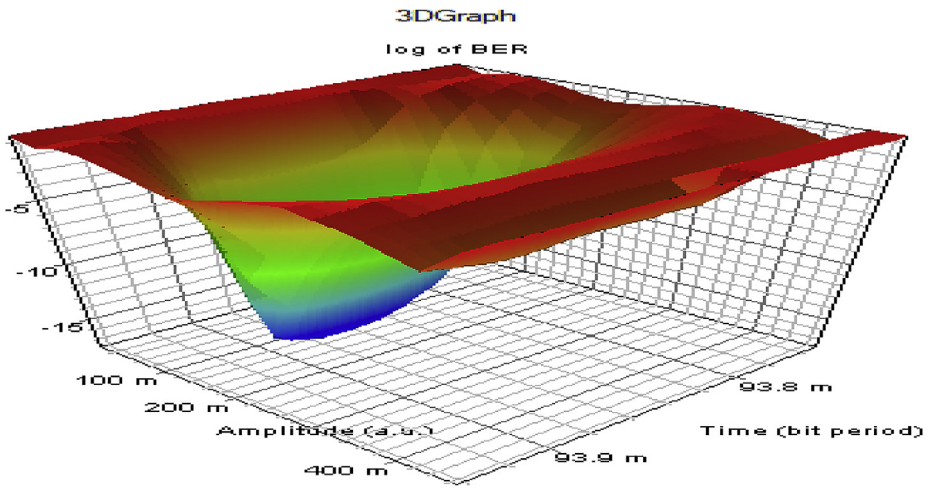

Figure 19. 3D graph of Time (bit period) versus Amplitude (a.u) versus BER of the Conventional SISO 1TX/RX FSO system under light fog condition.

and light fog attenuations, respectively, of the polarized quasi diffused system with power divider/hologram, the polarized system without hologram and the conventional SISO 1TX/RX FSO system. Also, from the figures, we can clearly see that the plots of the eye height (a.u) versus the link range (km) for the proposed polarized quasi diffused system with hologram/power divider under the three different atmospheric attenuations show a better performance metric compared to the polarized system without hologram/power divider and that of the conventional SISO 1TX/RX FSO system.

The 3D graphs in Figures 17, 18, and 19 show the systems' response (distortion pattern of the received signals) under light fog atmospheric attenuation over a desirably long transmission range. Hence, we can see that the proposed model with a power divider/hologram shows less received signal degradation (distortion) than that of the conventional SISO 1TX/RX system and the system without power divider/hologram. Therefore, the proposed model with power divider/hologram is promising in achieving better distortion less received signal for long transmission range than the conventional SISO 1TX/RX system.

5. Conclusion

Free space optics (FSO) is a guaranteed technology soon to break the limitations and challenges other wireless and fiber optic communication technologies face. However, atmospheric disturbances like aerosol (fog), scattering, turbulence, scintillation, etc., degrades the system performance of the high potential FSO links. The simulation results obtained for the polarized quasi-diffused FSO system model with power divider/holographic beam splitter, which serves as a spatial diversity scheme, show a much better performance improvement for an FSO link using one transmitter. A significant finding of this research is that maximum Q-factor, lower bit error rate (BER), and less transmission losses (considerably high received power) over suitable transmission range can be achieved under adverse atmospheric weather by using the polarized quasi diffused system with a power divider/holographic beam splitter without increasing the number of transmitters or receivers. Hence, the clear advantage of the polarized quasi diffuse model with power divider/holographic beam splitter is that it enables one transmitter to radiate optical signal along different polarization paths to minimize the effect of atmospheric disturbances. Therefore, we hope this research will serve as a valuable foundation contributing to the emerging FSO technologies in the future to prompt further efforts on the application of power divider/hologram to hybrid RF/FSO communication for 5G networks. It is known that the RF link can maintain reliable communication at a reduced data rate using the millimeter-wavelength carrier, and it is additionally less affected by foggy weather but highly prone to atmospheric effects like rain and scintillation. Whereas the FSO systems can provide a high data rate with advantages of reliable security, no frequency regulation, and quick deployment periods, its signal is also highly susceptible to atmospheric effects like fog, snow, etc. In that regard, applying power divider/hologram hybrid RF/FSO communication for 5G networks is promising. It will serve as a complementary focus for a better telecommunication system performance shortly.

Declarations

Author contribution statement

Abu Bakarr Sahr Brima: Conceived and designed the experiments; Performed the experiments; Analyzed and interpreted the data; Contributed reagents, materials, analysis tools or data; Wrote the paper.

Edwin Ataro & Aladji Kamagate: Analyzed and interpreted the data; Contributed reagents, materials, analysis tools or data; Wrote the paper.

Funding statement

This work was supported by the African Union through its Commission of Human Resources, Science and Technology (Pan African Institute for Basic Sciences, Technology and Innovation-PAUSTI), hosted in Kenya.

Data availability statement

Data included in article/supp. material/referenced in article.

Declaration of interests statement

The authors declare no conflict of interest.

Additional information

No additional information is available for this paper.

References

[1] M.N.O. Sadiku, S.M. Musa, S.R. Nelatury, Free space optical communications: an overview, Eur. Sci. J. 12 (9) (2016) 55.

[2] K.H. Shakthi Murugan, M. Sumathi, Design and analysis of 5G optical communication system for various filtering operations using wireless optical transmission, Results Phys. 12 (2019) 460–468.

[3] M.Z. Chowdhury, M.T. Hossan, A. Islam, Y.M. Jang, A comparative survey of optical wireless technologies: architectures and applications, IEEE Access 6 (2018) (2018) 9819–9840.

[4] J.S.B. Reeba Roy, Performance analysis of multiple TX/RX free space optical system under atmospheric disturbances, Int. J. Eng. Res. Technol. 4 (1) (2015) 445–447 [Online]. Available: www.ijert.org.
[5] S.M. Hamzah, I.A. Murdas, Enhancement of the performance of DWDM free space optics (FSO) communications systems under different weather conditions, Int. J. Intell. Eng. Syst. 13 (4) (2020) 446–456.
[6] A.E.A. Mohamed, A.N. Zaki, (FSO) systems using polarized DWDM-OFDM technique under atmospheric disturbances, 2017, pp. 8–13.
[7] X. Huang, et al., Performance comparison of all-optical amplify-and-forward relaying FSO communication systems with OOK and DPSK modulations, IEEE Photon. J. 10 (4) (2018) 1–11.
[8] Dr. Shehab, A. Kadhim, Dr. Salah Aldeen, A. Taha, P. Ali Q. Baki, Characterization study and simulation of MIMO free space optical communication under different atmospheric channel, IJISET -Int. J. Innov. Sci. Eng. Technol. Impact Factor 3 (8) (2016) 587–595 [Online]. Available: www.ijiset.com.
[9] A. Bekshaev, O. Orlinska, M. Vasnetsov, Optical vortex generation with a 'fork' hologram under conditions of high-angle diffraction, Opt Commun. 283 (10) (2010) 2006–2016.
[10] Z. Ghassemlooy, X. Tang, S. Rajbhandari, Experimental investigation of polarisation modulated free space optical communication with direct detection in a turbulence channel, IET Commun. 6 (11) (2012) 1489–1494.
[11] L.A. Romero, F.M. Dickey, Chapter 6 – the Mathematical Theory of Laser Beam-Splitting Gratings 54, Elsevier B.V., 2009, 10.
[12] Z. Ghassemlooy, S. Rajbhandari, W.O. Popoola, C.G. Lee, Coherent polarization shift keying modulated free space optical links over a gamma-gamma turbulence channel school of computing , optical communications research group , engineering and information Sciences, Northumbria Univ. UK Inst. Digi. 4 (4) (2011) 520–530.
[13] T. Set-up, et al., Beam splitter application notes 972, 2015, 8.
[14] X. Song, F. Yang, J. Cheng, N. Al-Dhahir, Z. Xu, Subcarrier phase-shift keying systems with phase errors in lognormal turbulence channels, J. Lightwave Technol. 33 (9) (2015) 1896–1904.
[15] M. Uysal, J. Li, M. Yu, Error rate performance analysis of coded free-space optical links over gamma-gamma atmospheric turbulence channels, IEEE Trans. Wireless Commun. 5 (6) (2006) 1229–1233.
[16] S. Mahajan, D. Prakesh, H. Singh, Performance analysis of free space optical system under different weather conditions, in: 2019 6th Int. Conf. Signal Process. Integr. Networks, SPIN 2019, 2019, pp. 220–224.
[17] M. Abaza, R. Mesleh, A. Mansour, E.H. Aggoune, Performance analysis of MISO multi-hop FSO links over lognormal channels with fog and beam divergence attenuations, Opt Commun. 334 (2015) 247–252.
[18] Optiwave, OptiSystem tutorial - volume 1 communication system design software, Opti Syst. 500 (2014) 1–500.
[19] S.A. Kadhim, A.H. Ali, K.M.A. Hussain, Simulation and comparative analysis of (SISO over MIMO) FSO communication channel, Int. J. Innov. Res. Sci. Eng. Technol. 6 (2017). November.